Acta Pharmaceutica Sinica B 2026;16(2):994−1008

Chinese Pharmaceutical Association
Institute of Materia Medica, Chinese Academy of Medical Sciences

Acta Pharmaceutica Sinica B

www.elsevier.com/locate/apsb
www.sciencedirect.com

ORIGINAL ARTICLE

Carboxylated prodrug of capsaicin with enhanced peripheral nerve permeation mediated by monocarboxylate transporters for long-lasting local anesthesia

Yu Wen[a,b], Tian Yang[a], Qi Li[a], Xiaosi Li[a], Xiaoyan Ma[a], Huiyang Hu[a], Prabhakar Busa[a], Sayma Alam[d], Libo Tan[d], Chao Zhao[a,b,c,e,*]

[a]*Department of Chemical and Biological Engineering, University of Alabama, Tuscaloosa, AL 35487, USA*
[b]*Department of Chemical and Biomolecular Engineering, University of Massachusetts Amherst, Amherst, MA 01003, USA*
[c]*Department of Biomedical Engineering, University of Massachusetts Amherst, Amherst, MA 01003, USA*
[d]*Department of Human Nutrition and Hospitality Management, University of Alabama, Tuscaloosa, AL 35487, USA*
[e]*Center for Convergent Biosciences and Medicine, University of Alabama, Tuscaloosa, AL 35487, USA*

Received 7 February 2025; received in revised form 17 August 2025; accepted 23 September 2025

KEY WORDS

Monocarboxylate transporter 1;
Local anesthetic;
Prodrug;
Capsaicin analogue;
TRPV1;
Nerve barrier penetration;
Sensory nerve blockade;
Long-lasting local anesthesia

Abstract Perineurally injected nerve-blocking agents have limited capability to cross peripheral nerve barriers (PNBs), requiring high doses to block pain signals on axons. This increases the risk of local tissue toxicity and systemic side effects on the cardiovascular and neurological systems. To address this, we explored carboxyl group modification to enhance the permeability of nerve-blocking agents across the PNBs through carrier-mediated transport facilitated by monocarboxylate transporters (MCTs). The enhanced permeability allows for targeted drug delivery to peripheral nerve axons, resulting in a significant reduction in the necessary drug dosage for a long-lasting nerve block. Specifically, we developed a carboxylated prodrug of capsaicin (COOH-CAP) by conjugating it with a carboxyl group *via* a degradable ester bond. Calcium flux assays, patch-clamp recordings, and body temperature measurements collectively confirmed that COOH-CAP activates TRPV1, with potency comparable to capsaicin. In rats, a single sciatic nerve injection of 3.28 μmol COOH-CAP produced a nociceptive-selective nerve

*Corresponding author.
E-mail addresses: chaozhao@umass.edu, czhao15@eng.ua.edu (Chao Zhao).

Peer review under the responsibility of Chinese Pharmaceutical Association and Institute of Materia Medica, Chinese Academy of Medical Sciences.

https://doi.org/10.1016/j.apsb.2025.11.006

blockade lasting 260 ± 83.7 h without motor impairment or capsaicin-related side effects, approximately 35 times longer than the same dose of plain capsaicin. Even at a lower dose of 1.64 μmol, COOH-CAP still produced nociceptive-selective nerve blockade for 172.0 ± 41.3 h.

1. Introduction

Approximately 300 million major surgeries were performed globally in 2023, with around 75% of these patients experienced moderate to severe acute postoperative pain[1,2]. Postoperative pain presents a significant challenge to healthcare systems and patient satisfaction. Opioid analgesics, long regarded as the mainstay for managing moderate to severe postoperative pain, are increasingly problematic due to their potential for misuse, dependence, and addiction, fueling the ongoing opioid crisis[3]. Local anesthesia, which involves injecting local anesthetics around peripheral nerves to relieve pain, is a common worldwide practice for postoperative pain management[4]. Local anesthetics work by blocking neuronal voltage-gated sodium channels (VGSCs) and interrupting nerve impulse propagation. Despite the effectiveness in nerve block, the duration of action of clinically used amino-ester and amino-amide local anesthetics typically limited to a few hours[5]. To extend the duration of the nerve block, perineural catheters, adjuvant drugs, or sustained release systems, such as liposomes or nanoparticles can be used[6-12]. However, clinically used amino-ester and amino-amide local anesthetics are intrinsically myotoxic[13,14], leading to muscle weakness, poor physical stamina, and lack of muscle control, particularly with prolonged use or high doses[15]. Additionally, once these local anesthetics are cleared from the injection site, they can have systemic effects, potentially causing cardiac dysfunction and neurological syndromes such as seizures[9,16].

The limited duration of action and prevalence of side effects in peripherally injected local anesthetics can be attributed to their low bioavailability to peripheral nerve axons. Peripheral nerve axons are surrounded by peripheral nerve barriers (PNBs), which include the epineurium, perineurium, and endoneurium. Among these, the perineurium—a concentric layer of fibroblasts that encloses bundles of nerve fibers, is the major obstacle that local anesthetics must overcome to permeate from the perineural injection site and diffuse towards their intended site of action[17,18]. It is widely recognized that only a very small percentage (<1%) of perineurally injected local anesthetics can penetrate the perineurium and effectively modulate axonal impulse conduction[17]. The majority of these local anesthetics are instead absorbed by nearby tissues or enter the systemic circulation, leading to off-target effects and potential drug toxicity both locally and systemically.

Monocarboxylate transporters (MCTs) are encoded by the *SLC16A* gene family and have 14 subtypes, MCT1-14[19,20]. Endothelial cells that form the blood−brain barrier (BBB) express MCTs, with monocarboxylate transporter 1 (MCT1) being the most prevalent. MCT1 has a moderate affinity for lactate ($K_m \approx 3.5$ mmol/L) and can recognize aliphatic monocarboxylates with carbon chain lengths of 2 to 5. This allows for the transport of monocarboxylates in and out of cells that have high MCT1 expression under physiological conditions[21,22]. MCT1 facilitates the transport of a broad range of monocarboxylate solutes across the BBB, including lactate, pyruvate, and acetoacetic acid, through a carrier-mediated mechanism[22-24]. Previous studies have also shown that certain carboxylate drugs, such as valproic acid, benzoic acid, nicotinic acid, and β-lactam antibiotics like benzylpenicillin, propicillin, and cefazolin can be transported into the brain *via* MCT1[25-27]. Importantly, MCT1 is also expressed in multiple cell types within peripheral nerves, including the endothelial cells of endoneurial blood vessels, Schwann cells, and perineurial (glial) cells[28]. In peripheral nerves, MCT1 is believed to mediate the transport of monocarboxylate solutes across the restrictive PNBs[28-31]. Furthermore, Schwann cells express additional monocarboxylate transporters, such as MCT2 and MCT4, suggesting that multiple MCT isoforms contribute to intracellular transport and metabolic exchange within the peripheral nerve microenvironment[28].

In this study, we developed a carboxylated prodrug of nerve-blocking agents by linking nerve-blocking agents with a carboxyl group through degradable ester bond (Scheme 1). We hypothesize that the MCT1 present on the perineurium facilitates the transport of prodrug through the perineurium. Once the prodrug has permeated the nerve, they are converted to their active parent drug through the hydrolysis of chemical bonds. This transportation mechanism significantly increases the drug availability to peripheral nerve axons. The increased drug availability allows a higher proportion of the administered drug to produce the desired nerve block, offering equivalent or superior pain relief effects with lower side effects at equal or lower drug doses.

Capsaicin was selected as the nerve-blocking agent. As an active component extracted from chili peppers, capsaicin is clinically used as a topical treatment of neuropathic pain[32]. Unlike traditional local anesthetics, capsaicin is not classified as a local anesthetic due to its distinct mechanism of action[33]. It specifically binds to and activates the transient receptor potential vanilloid 1 (TRPV1) receptor[34]. Prolonged stimulation of TRPV1 can lead to receptor desensitization, thereby alleviating pain. Since TRPV1 is primarily expressed at the peripheral terminals of sensory neurons, capsaicin can produce a selective nociceptive nerve block without causing significant motor impairment[35,36]. The concept of selective nociceptive/nociceptor analgesia was first introduced by Jancsó et al.[37] in 1980, who provided direct evidence for an axonal site of action of capsaicin. Since then, perineural capsaicin application has become a widely used experimental approach to investigate the function of TRPV1-positive primary sensory neurons, and its potential use in pain therapy has also been proposed[38-45]. However, high-doses of capsaicin have been reported to potentially cause side effects such as inflammation, neurotoxicity, seizures, shortness of breath, and strong irritant effects, while the selective axonal blockade of low-doses capsaicin has a shorter duration[46,47]. These concerns limit its broader application. The enhancement of the effectiveness of capsaicin in nerve blocks would have a significant impact on clinical practice.

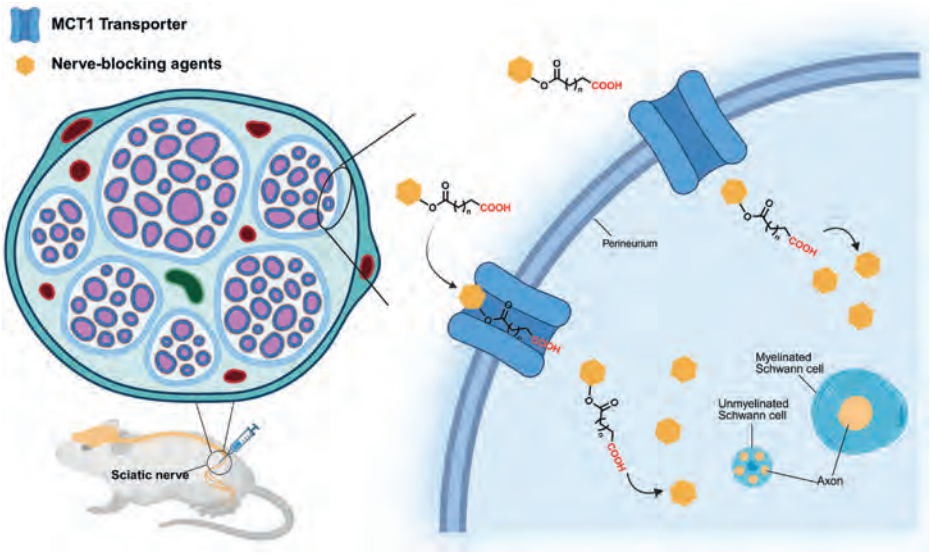

Scheme 1 Carboxylated prodrug of nerve-blocking agents penetrate the peripheral nerve barrier mediated by the MCT1 transporter and act on sensory neurons.

2. Results

2.1. MCT1 transporter-mediated carboxyl group-containing fluorescein endoneurial permeation in vivo

We utilized a rat sciatic nerve permeation model to investigate whether the MCT1 transporter can facilitate the permeation of carboxyl group-containing drugs into peripheral nerves. Previous studies have shown that peripherally injected fluorescein isothiocyanate (FITC) cannot cross the perineurium[48,49]. In this study, we studied whether the peripherally injected 5-carboxyfluorescein (5-FAM), an analog of FITC containing a carboxyl group, can cross the perineurium (Fig. 1A). As a control, we assessed the permeability of 5-aminofluorescein (5-AFM), an amino-substituted analogue of FITC, following peripheral administration. In addition, as a negative control, we co-administered 5-FAM with the MCT1 inhibitor α-cyano-4-hydroxycinnamate (CHC), referred to as 5-FAM@CHC, around the rat sciatic nerve. CHC is a well-characterized inhibitor of MCT1−4 that interacts with the active site of MCT proteins, thereby impairing their transport function[22].

Adult male Sprague−Dawley (SD) rats weighing 250−350 g were injected with 0.3 mL of phosphate-buffered saline (PBS, 1 × , pH 7.4) solution containing equimolar amounts (15.6 μmol/L) of FITC, 5-FAM, 5-AFM, or 5-FAM@CHC around the sciatic nerve. Four hours after injection, the rats were euthanized, and the sciatic nerve and surrounding tissue were collected, cryosectioned, and observed using confocal microscopy.

As shown in Fig. 1B, fluorescence was not observed in the endoneurium of the peripheral nerve in rats injected with FITC. This indicates that FITC could not penetrate the perineurium to enter the endoneurium of the sciatic nerve. Instead, FITC accumulated in adjacent muscle tissue and adipose tissue around the sciatic nerve. In rats injected with 5-AFM, fluorescence was faintly observed within the endoneurium. This indicates that the introduction of the amino group in 5-FAM improved the ability of FITC to penetrate the sciatic nerve perineurium to some extent. One possible explanation for this improvement could be the presence of glutamate transporter in the perineurium[50]. In contrast, in rats injected with 5-FAM, fluorescence distributed evenly both inside and outside the sciatic nerve perineurium. There was no accumulation of fluorescein in the surrounding muscle tissue and adipose tissue. Furthermore, co-injection of 5-FAM with the MCT inhibitor CHC (5-FAM@CHC) resulted in fluorescence signals primarily localized to the surrounding muscle and adipose tissues, with minimal signal detected within the nerve. This observation indicates that the transperineurial penetration of 5-FAM is largely dependent on MCT1-mediated transport.

Quantitative analysis revealed that the average relative fluorescence intensity within the endoneurium of the sciatic nerve was significantly higher in rats injected with 5-FAM compared to those injected with FITC, 5-AFM, or 5-FAM@CHC, with statistically significant differences observed (Fig. 1C and D). These results indicate that MCT1 can effectively transport carboxyl-containing fluorescein, injected peripherally, across the perineurium and into the endoneurium of the peripheral nerve.

2.2. Synthesis and characterization of the COOH-CAP prodrug

We designed the carboxylated capsaicin prodrug (COOH-CAP, 1) by introducing the succinyl group to capsaicin through degradable ester bond (Fig. 2A). The reason for choosing succinylation is that after the COOH-CAP prodrug hydrolyze in tissues, they form the parent drugs and succinic acid by-products. Succinic acid is a naturally occurring acid that is widely present in animal and plant tissues, as well as microorganisms, and is considered a non-toxic acid[51-53].

The synthesis of the COOH-CAP prodrug was achieved by condensing the phenolic hydroxyl group of commercially available natural capsaicin (capsaicin: dihydrocapsaicin ratio of approximately 3:1) with the carboxyl group of succinic anhydride using 4-dimethylaminopyridine (DMAP) as a catalyst and pyridine as a base at room temperature (Fig. 2B). The chemical shifts of the methylene groups in the succinyl moieties of the prodrug were readily identified in the range of 2.5−3.1 ppm by ^{1}H NMR (Fig. 2C and Supporting Information Fig. S1). Additionally,

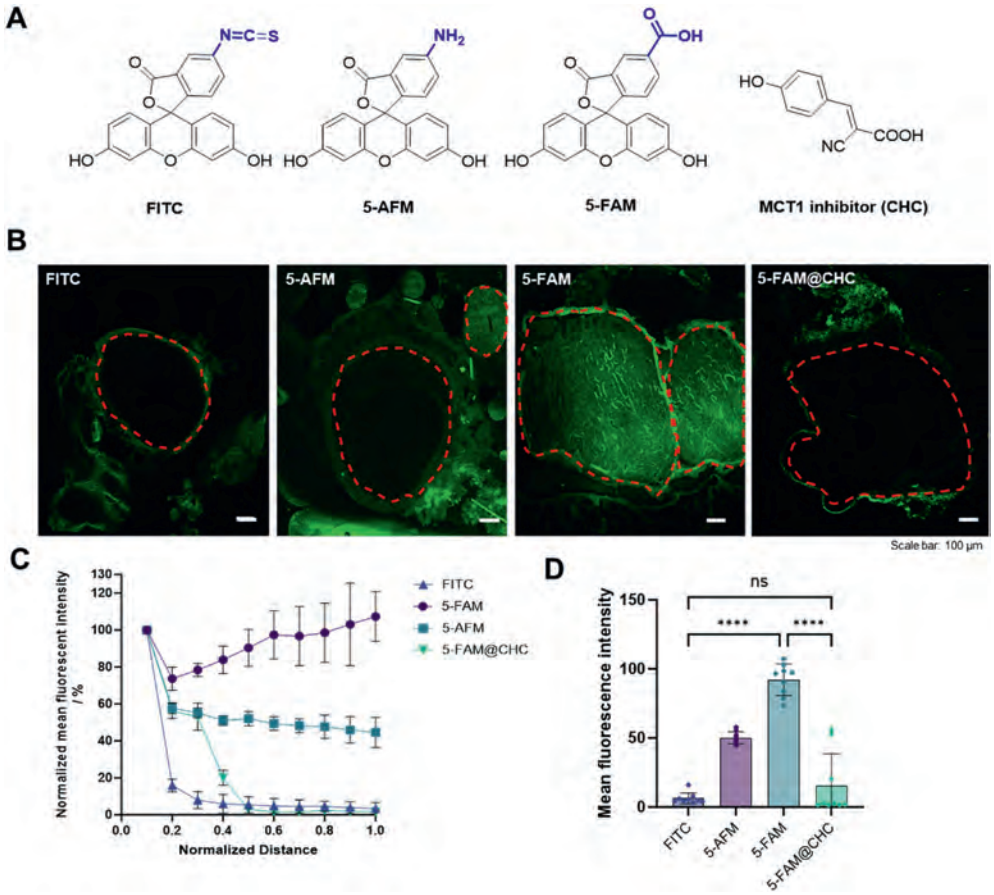

Figure 1 *In vivo* peripheral nerve permeability. (A) Structure of FITC, 5-FAM, 5-AFM, and CHC. (B) Representative fluorescent photomicrographs of sciatic nerves and surrounding epineurium 4 h after perineural injection of FITC, 5-AFM, 5-FAM, and 5-AFM@CHC. The red dotted line indicates the perineurium. (C) Relationship between normalized mean fluorescence intensity and normalized distance from the surface of the nerve in rats injected with FITC, 5-FAM, 5-AFM, and 5-AFM@CHC. (D) Mean fluorescence intensity in the endoneurium of sciatic nerves injected with FITC, 5-AFM, 5-FAM, or 5-FAM@CHC. Data are presented as mean ± SD ($n = 3$). One-way ANOVA followed by Tukey's test; ****$P < 0.0001$, ns: not significant.

through Q-TOF high-resolution mass spectrometry (HRMS), we successfully identified a peak corresponding to COOH-CAP bound to sodium ions ($[\text{COOH-CAP} + \text{Na}]^+ = 428.2039$), further confirming the structure of the compounds (Fig. 2D).

Hydrolysis kinetics of the prodrug were evaluated in deionized (DI) water at 37 °C. A suspension of 5 mg of prodrug in 10 mL of DI water was placed in an incubator at 37 °C. Samples were taken every hour, and the hydrolysis products of the prodrug were analyzed using UPLC. The hydrolysis experiments showed successful conversion of the COOH-CAP prodrug into their corresponding parent drugs capsaicin (Fig. 2E). The COOH-CAP prodrug could be completely degraded within 30 h, with a half-life of 3.94 h (Fig. 2F). Furthermore, a separate metabolic study in rat sciatic nerve homogenate revealed a markedly accelerated degradation rate, with a calculated half-life of 38 min, suggesting enzyme-mediated hydrolysis of the prodrug (Supporting Information Fig. S2). Notably, in this *in vitro* model, the enzyme concentration is much higher than that in the actual local physiological conditions where the prodrug is administrated. Specifically, approximately 1 cm segments of sciatic nerve were homogenized in 1 mL of 1 × PBS, leading to the complete release and uniform dispersion of intracellular and membrane-associated enzymes. In clinical or experimental nerve block settings, however, the prodrug is delivered into the perineural extracellular space, where enzymatic activity is more spatially restricted and diffusion-limited. As such, the half-life of prodrug hydrolysis after *in vivo* injection around the sciatic nerve should be much longer than 38 min.

2.3. Evaluation of TRPV1 activation of the COOH-CAP prodrug

To assess the TRPV1-activating potential of COOH-CAP, a calcium flux assay was performed in human HEK293 cells expressing TRPV1[54,55]. COOH-CAP induced a concentration-dependent activation of TRPV1, with an EC_{50} value of 2.96 nmol/L, which is comparable to that of capsaicin (3.73 nmol/L, $P = 0.16$) (Fig. 3A). To corroborate these results, whole-cell manual patch-clamp recordings were conducted using the same TRPV1-expressing HEK293 cells. COOH-CAP elicited robust inward currents in a dose-dependent manner, with an EC_{50} of 449 nmol/L, closely matching that of capsaicin (408 nmol/L, $P = 0.08$)

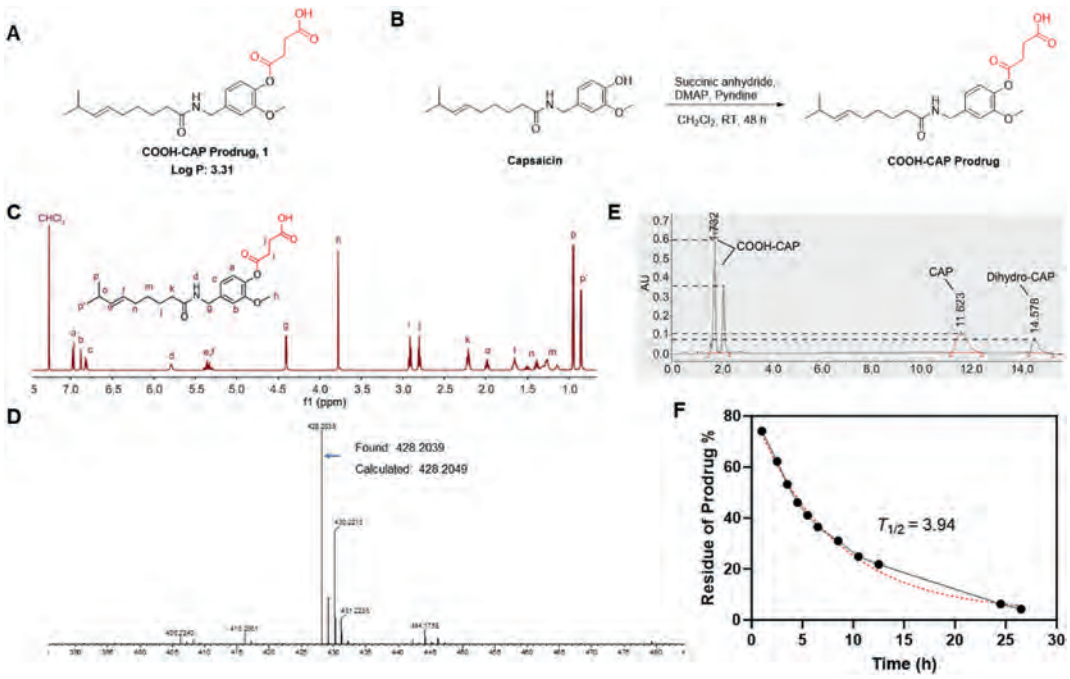

Figure 2 Synthesis route and characterization of the COOH-CAP prodrug. (A) Structure of the COOH-CAP prodrug. (B) Synthesis route of the COOH-CAP prodrug. (C) ^{1}H NMR (500 MHz) spectrum of the COOH-CAP prodrug. (D) HRMS signal spectrum for COOH-CAP prodrug. (E) UPLC chromatography illustrated that the COOH-CAP prodrug was partially degraded to capsaicin after 1 h. (F) Hydrolysis kinetics of COOH-CAP prodrug in DI water at 37 °C determined by UPLC.

(Fig. 3B−D). These findings confirm that COOH-CAP activates TRPV1 through direct electrophysiological stimulation. The comparable *in vitro* potency of COOH-CAP and capsaicin may be attributed to the membrane-associated esterases on HEK293 cells or, more likely, to intracellular esterases, given the MCT1-mediated uptake of COOH-CAP, These esterases facilitate rapid convertion of COOH-CAP to capsaicin during the assay[72,73].

To further evaluate its functional relevance *in vivo*, we measured core body temperature in rats after an intraperitoneal injection of COOH-CAP (0.16 μmol in 100 μL 1 × PBS). A transient hypothermic response was observed, with the temperature dropping to 35.3 ± 0.4 °C at 15 min and gradually returning to baseline (36.9 ± 0.1 °C) by 120 min (Fig. 3E). An equivalent molar dose of capsaicin produced a similar hypothermic profile, reaching 35.6 ± 0.3 °C at 30 min, followed by recovery to 36.8 ± 0.2 °C at 45 min, confirming that COOH-CAP has the same thermoregulatory effects as capsaicin.

To verify whether the hypothermic effect of COOH-CAP was mediated through TRPV1 activation, we employed a pharmacological antagonist reversal strategy. Rats were first injected with COOH-CAP (0.16 μmol), followed 30 min later by the TRPV1 antagonist AMG9810 (5 mg in 0.3 mL 1 × PBS, intraperitoneally). Administration of AMG9810 rapidly reversed the COOH-CAP-induced hypothermia, elevating body temperature to 37.9 ± 0.3 °C at 45 min and stabilizing at 37.4 ± 0.1 °C by 60 min (Fig. 3F). This pharmacological reversal indicates that the hypothermic response to COOH-CAP is TRPV1-dependent, further confirming its target-specific mechanism of action.

2.4. *Sciatic nerve blockade induced by COOH-CAP prodrug*

The rat sciatic nerve block model is commonly used to evaluate the efficacy and safety of local anesthetics[49,56-58]. We selected SD rats (250−350 g) and injected PBS solutions containing different doses of the COOH-CAP prodrug (0.82, 1.64, and 3.28 μmol) along with 7.5 mg of Tween 20 above the left sciatic nerve. Tween 20 was included to enhance the solubility of the prodrug for injectable formulation[59]. After injection, neurobehavioral tests were conducted to assess the functional deficits of the treated rats' hind paws, including the nociceptive axonal blockade (using a hot plate test to measure the tolerance time of both hind paws, with a thermal response time greater than 7 s indicating nociceptive axonal blockade) and motor axonal blockade (using a balance to measure the maximum weight borne by both legs). Additionally, capsaicin-related side effects, such as contralateral nociceptive axon blockade in the uninjected right hind limb, irreversible nociceptive axon blockade, seizures, and rapid breathing, were observed post-injection. Data from a related animal experiment using plain capsaicin as a control compound were previously obtained in our laboratory and have been published[49].

Compared to plain capsaicin, the COOH-CAP prodrug exhibited enhanced effectiveness in nociceptive axonal blockade. Injections of a low dose (0.82 μmol) of the COOH-CAP prodrug and plain capsaicin did not block the nociceptive axons of the rat sciatic nerve (Fig. 4A and B, Supporting Information Fig. S3). However, when the dose of the COOH-CAP prodrug was increased to only 1.64 μmol, all treated rats experienced complete blockade of nociceptive axons on the injection side, which lasted for 172.0 ± 41.3 h. In contrast, the same dose of plain capsaicin only achieved successful nociceptive axonal blockades in all treated rats for 2.0 ± 2.8 h (Fig. 4A and B, Supporting Information Fig. S4). When the dose of the COOH-CAP prodrug was further increased to 3.28 μmol, the duration of nociceptive axonal blockade on the injected side reached 260.0 ± 83.7 h. As a comparison, the same dose or even a higher dose (6.54 μmol) of plain capsaicin only achieved successful blockade for 6.8 ± 6.1

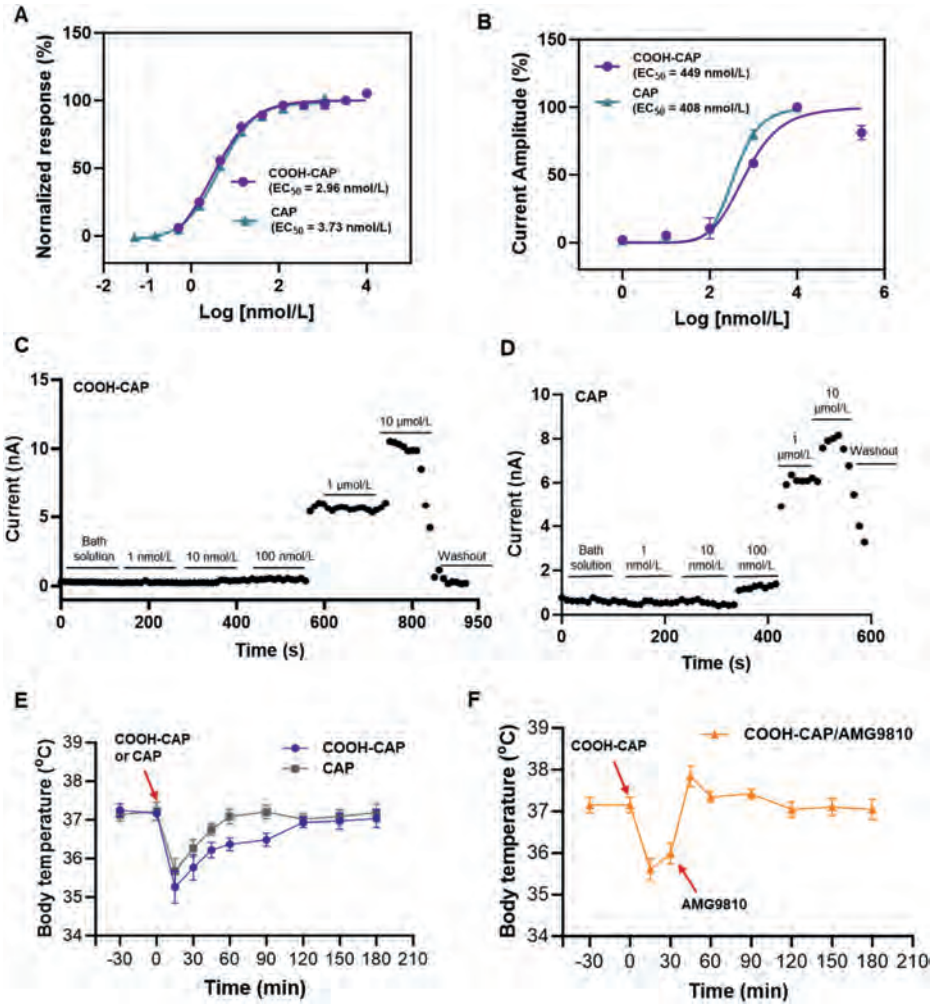

Figure 3 TRPV1 activation and hypothermic responses induced by COOH-CAP and capsaicin. (A) Dose−response curves of COOH-CAP and capsaicin measured by calcium flux assay in HEK293 cells stably expressing human TRPV1. The fluorescence response induced by 1 μmol/L capsaicin was set as 100%. (B) Concentration−response curves obtained from manual whole-cell patch-clamp recordings in the same TRPV1-expressing HEK293 cells. Current amplitudes were normalized to the response elicited by 10 μmol/L capsaicin. (C, D) Representative whole-cell patch-clamp traces showing inward currents evoked by sequential application of increasing concentrations of COOH-CAP or capsaicin. Data are presented as mean ± SD. from a representative experiment performed in triplicate. EC_{50} values were calculated using nonlinear regression fitting to the Hill equation. (E) Core body temperature changes in rats following intraperitoneal injection of COOH-CAP (0.16 μmol in 100 μL 1 × PBS) or CAP (0.16 μmol in 100 μL 1 × PBS). (F) AMG9810, a selective TRPV1 antagonist, reversed the hypothermic effect of COOH-CAP. In a separate cohort, rats were first injected with COOH-CAP (0.16 μmol in 100 μL 1 × PBS), followed by AMG9810 (5 mg, intraperitoneally) at 30 min. Data are presented as mean ± SEM (n = 6 per group).

and 4.0 ± 2.0 h, respectively (Fig. 4A and B, Supporting Information Fig. S5). Consistent with previous reports using the same doses of capsaicin (0.82, 1.64, or 3.28 μmol), neither contralateral antinociceptive effects nor other capsaicin-related side effects were observed following the perineural injection of either capsaicin or the COOH-CAP prodrug (Supporting Information Figs. S3−S6). Furthermore, a single injection of 0.82, 1.64 and 3.28 μmol of the COOH-CAP prodrug did not cause motor nerve block and capsaicin-related side effects, such as nociceptive axon blockade on the contralateral side, seizures, and rapid breathing (Fig. S6). After 28 days, in all rats received the injection of COOH-CAP prodrug, the thermal response duration on the injected side returned to baseline levels, and the maximum weight-bearing capacity of both hind limbs and paws remained normal (Figs. S3−S6). These results indicate that effective doses of COOH-CAP prodrug injection do not produce irreversible nerve block, which is a common side effect of high-dose capsaicin and its analogs[42,47].

The discovery of a long-acting nerve block that selectively blocks the sensory fibers is highly desired. It will decrease the need for opioids postoperatively significantly and reduce the problems related to that. Performing nerve blocks for pain control usually does not differentiate between the sensory and motor fibers. Blocking the motor nerves is undesirable, as it will delay ambulation, recovery, and hospital discharge.

2.5. *Tissue reaction*

To evaluate the tissue reaction to COOH-CAP prodrug, we euthanized rats 14 or 28 days after injecting COOH-CAP. We collected muscle tissue and nerves near the injection site around the sciatic nerve. We then stained and observed the

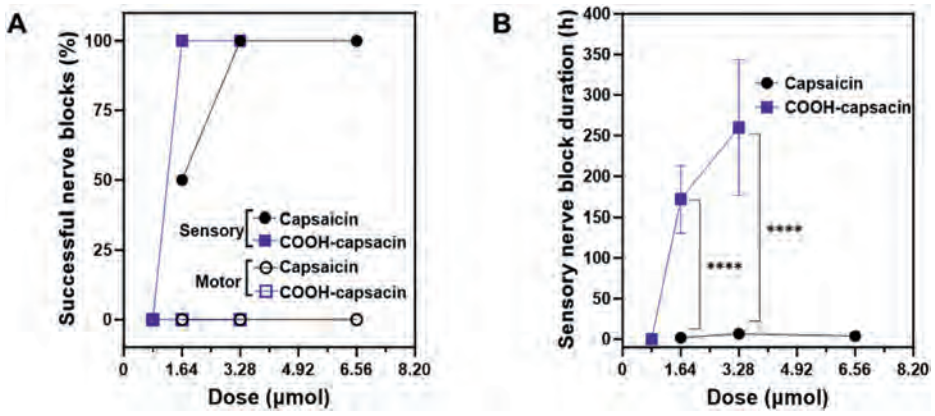

Figure 4 Sciatic nerve blockade with plain capsaicin and COOH-CAP prodrug. Effects of drug dose on (A) frequency of successful nociceptive axon and motor axon blockade and (B) duration of nociceptive axon blockade. Data are presented as mean ± SD ($n = 6$). One-way ANOVA followed by Tukey's test; ****$P < 0.0001$.

muscle and nerve sections using hematoxylin and eosin (HE) staining and toluidine blue staining, and quantified myotoxicity and inflammation using a previously reported scoring system [60].

As shown in Fig. 5, 14 or 28 days after injecting 0.82, 1.64, and 3.28 μmol of COOH-CAP in rats, there was no edema or discoloration in the surrounding tissues, nor were there any obvious signs of tissue damage. Further microscopic examination revealed no significant myotoxicity or inflammation in the tissues surrounding the sciatic nerve (scores ranged from 0 to 1) (Table 1).

Observation of toluidine blue-stained sections revealed that the nerve fibers in the rats injected with the COOH-CAP prodrug were tightly arranged and encased by round or oval myelin sheaths. There were no significant changes in axon density or myelin structure across the groups, indicating that the injection of both

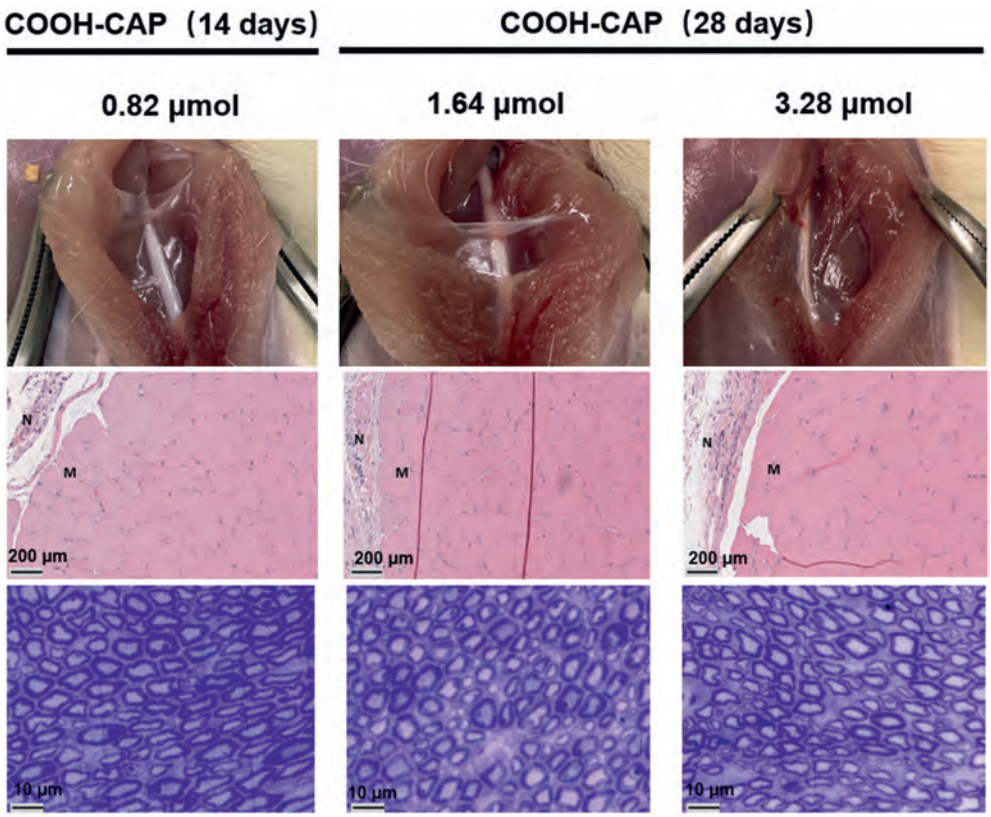

Figure 5 Tissue reaction to COOH-CAP 14 or 28 days after sciatic nerve injection. Representative photographs of the dissected injection site, followed by representative H&E-stained thick sections of muscles and adjacent loose connective tissue, and toluidine blue-stained semi-thin epon-embedded sciatic nerve sections are shown. N: epimysial connective tissue, M: muscle. Scale bar: 200 and 10 μm.

Table 1 Myotoxicity and inflammation scores.

Group	Inflammation score	Myotoxicity score
COOH-CAP prodrug, 0.82 μmol	0 (0−1)	0 (0−0)
COOH-CAP prodrug, 1.64 μmol	0.5 (0−1)	0 (0−1)
COOH-CAP prodrug, 3.28 μmol	1 (0−1)	0.5 (0−1)

Note: Inflammation score range: 0−4; myotoxicity score range: 0−6. Data for inflammation and myotoxicity are medians and ranges, and are compared using the unpaired Mann−Whitney U test. This method was selected because the data were ordinal.

prodrugs did not cause noticeable nerve damage (Fig. 5). It is reported that high doses of capsaicin and its analogs may cause degeneration of unmyelinated C-fiber and prolonged activation of TRPV1 channels may result in irreversible calcium ion influx, leading to C-fiber swelling[61]. We used TEM to examine the sciatic nerve sections of rats injected with 3.28 μmol of COOH-CAP prodrug. Compared to untreated rats[49], the diameters of both myelinated fibers and unmyelinated C-fiber in COOH-CAP prodrug treated rats did not significantly increase, which may be attributed to the lower injection dose and slow hydrolysis of the prodrug (Fig. 6A and B, Supporting Information Fig. S7).

2.6. Enhanced nerve-blocking efficacy due to facilitated MCT1 transport

We hypothesize that the enhanced efficacy of the prodrug in nerve blockade is due to that the carboxyl group enhances prodrug permeability across the restrictive PNBs *via* carrier-mediated transport by the facilitative MCT1. To confirm this hypothesis, we designed a negative control Valeryl-capsaicin (Valeryl-CAP) prodrug. Unlike the COOH-CAP prodrug, Valeryl-CAP lacks a carboxyl group while preserving the same atomic length ($n = 5$) (Fig. 7A). Using commercially available capsaicin and valeryl chloride as starting materials, we successfully obtained the target product Valeryl-CAP through amide condensation (see Supporting Information Scheme S1 and Figs. S8−S10). Animal experiments showed that rats receiving a single injection of 1.64 μmol Valeryl-CAP prodrug produced nerve blockade in only 67% of the rats, lasting for 1.2 ± 1.0 h ($P < 0.0001$ *vs.* COOH-CAP alone) (Fig. 7B−D, E, and Supporting Information Fig. S11). In contrast, an equivalent dose of the COOH-CAP prodrug induced a nociceptive nerve blockade in all treated rats, with a duration of 172.0 ± 41.3 h.

To further validate the role of MCTs in facilitating the translocation of prodrugs across the PNBs, the prodrug was co-injected at the rat sciatic nerve with the CHC. CHC exhibits moderate inhibitory activity on human and rat MCT1 *in vitro* ($K_m = 425$ μmol/L)[22]. It is expected that adding CHC to the COOH-CAP prodrug injection solution will reduce MCT1 transport activity, thereby inhibiting the transport of the COOH-CAP prodrug across the PNBs. Rats that received a single injection of 1.64 μmol COOH-CAP prodrug and 400 μmol/L CHC in 0.3 mL PBS buffer showed a significantly shorter duration of nociceptive axon blockade, lasting only 1.5 ± 2.3 h ($P < 0.0001$ *vs.* COOH-CAP alone). In contrast, rats injected with 1.64 μmol COOH-CAP prodrug alone experienced a duration of nociceptive axon blockade lasting 172.0 ± 41.3 h, nearly 80 times longer (Fig. 7C−E and Supporting Information Fig. S12).

These results confirmed our hypothesis that MCTs promote the permeation of COOH-CAP prodrug into the nerves through a carrier-mediated transport mechanism, which consequently increases their effectiveness in blocking nerves.

Regarding the observation of a short-term thermal response in some rats treated with Valeryl-CAP or COOH-CAP in the presence of the MCT1 inhibitor CHC, we propose the following explanation: at a dose of 1.64 μmol, both Valeryl-CAP and COOH-CAP (even in the presence of the MCT1 inhibitor CHC) can function as ordinary prodrugs. Although these compounds cannot utilize MCT1 to cross the perineurium, they can passively diffuse across the perineurium, similar to plain capsaicin and local anesthetics. Moreover, previous studies[49] have shown that 1.64 μmol of free capsaicin alone can produce nerve blockade in approximately 50% of rats even without the aid of transporter-mediated uptake. This suggests that even limited passive diffusion of Valeryl-CAP and COOH-CAP allows them to enter the nerve, where they are subsequently hydrolysis to release free capsaicin, and cause the short-term anesthetic effect.

2.7. Enhanced nerve-blocking efficacy due to sustained release of capsaicin from the inactive prodrug

We hypothesize that, compared to capsaicin, the COOH-CAP prodrug are either inactive or less effective in nerve block. Following prodrug transport across PNBs, the inactive or less effective prodrug is gradually converted to active drug through

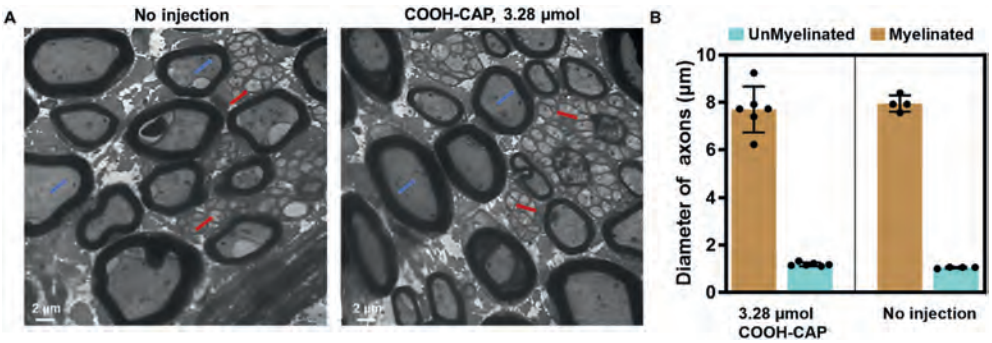

Figure 6 Representative TEM images of dissected sciatic nerves (A) and the diameter of myelinated fibers and unmyelinated C-fibers (B) 28 days post-injection of 3.28 μmol COOH-CAP prodrug. Red arrows denote unmyelinated C-fibers and blue arrows denote myelinated A-fibers. Scale bar: 2 μm. $n = 200$ fibers for diameter measurement (from 6 rats). Data are mean ± SD.

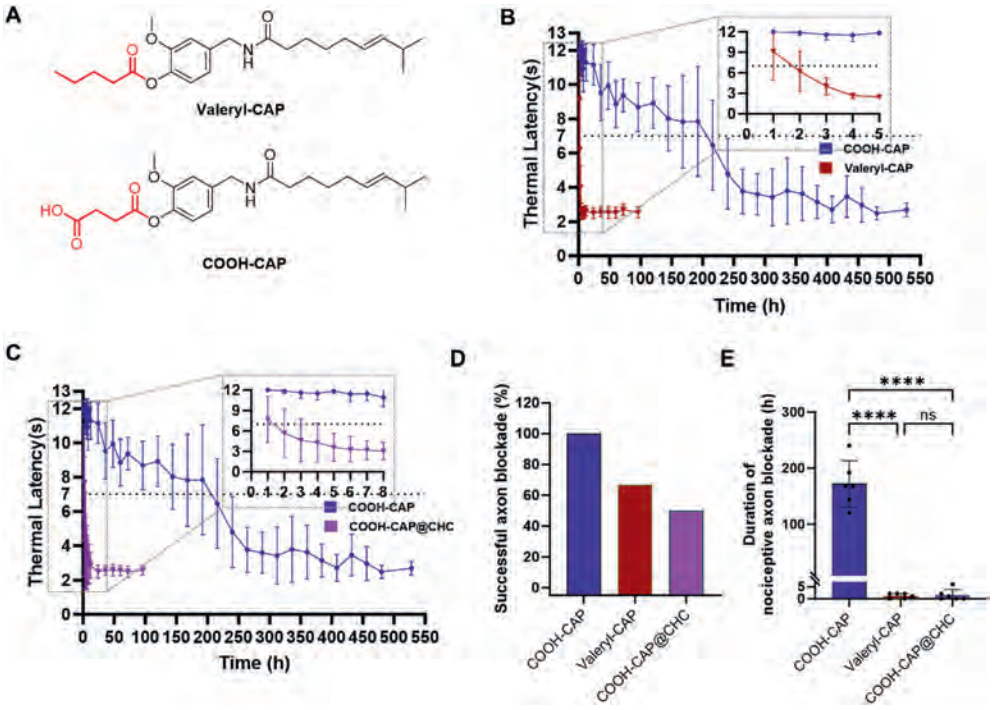

Figure 7 Effect of MCT inhibitor and absence of carboxyl group on the prodrug's nerve-blocking efficacy. (A) Chemical structures of Valeryl-CAP and COOH-CAP prodrugs. (B) Comparison of ipsilateral thermal latencies in rats' post-administration with 1.64 μmol Valeryl-CAP and COOH-CAP prodrugs. (C) Ipsilateral thermal latencies following injection of 1.64 μmol COOH-CAP with or without 400 μmol/L CHC. (D) Percentage of rats with successful axon blockade. (E) Duration of nociceptive axon blockade. Data are presented as mean ± SD ($n = 6$). One-way ANOVA followed by Tukey's test; ****$P < 0.0001$, ns: not significant.

linker hydrolysis, leading to sustained drug release. This sustained drug release also contributes to enhanced efficacy of the prodrug in nerve blockade. To study whether the prodrug itself has a nerve-blocking effect, we designed a negative control compound, carboxylated-ether-capsaicin (COOH-*O*-CAP), in which the carboxyl region and the CAP region are bound by the ether bond (Fig. 8A). Ether bond is not hydrolysable and can prevent dissociation of the prodrug in local tissues. Specifically, COOH-*O*-CAP was synthesized from capsaicin and methyl 4-bromobutanoate through nucleophilic substitution reaction and hydrolysis of ester group to carboxyl group (see Methods, Supporting Information Scheme S2 and Figs. S13−S15).

Animal experiment results showed that rats injected with 3.28 μmol of COOH-*O*-CAP did not experience sciatic nerve blockade (Fig. 8B and Supporting Information Fig. S16). In contrast, the same dose of COOH-CAP prodrug caused axonal blockade, lasting 260.0 ± 83.7 h. This result indicates the COOH-CAP prodrug itself has no nerve blocking effect until it is hydrolyzed into active capsaicin (Fig. 8C).

Molecular docking studies confirmed that the COOH-CAP prodrug does not possess TRPV1 agonist activity. The published crystal structure of the TRPV1-CAP complex (PDB: 7LPE) was used[62]. Docking calculations were performed using AutoDock Vina, and PyMOL 2.5 was used for visualization. As shown in Fig. 8D, capsaicin can successfully dock into the TRPV1 drug-binding pocket. The benzene ring of capsaicin can form a $\pi-\pi$ stacking interaction with the benzene ring of the Y511 residue in TRPV1, and the carbonyl group of the amide forms a hydrogen bond with the phenolic hydroxyl group of Y511. In contrast, although the compound COOH-*O*-CAP can be successfully docked into the TRPV1 drug-binding pocket, it cannot form $\pi-\pi$ stacking and hydrogen bonding interaction with the Y511 residue (Fig. 8E).

2.8. Reduced irritancy and lowered mechanical hypersensitivity induced by the COOH-CAP prodrug

High levels of irritancy, including sensations of burning and pain, are significant obstacles to the broader clinical application of capsaicin[63]. This irritation can lead to secondary harm to patients[64,65]. Previous studies have shown that this pungency is not determined by TRPV1 agonist potency, but is instead strongly associated with the compound's lipophilicity[66]. Lipophilicity influences the activation kinetics of TRPV1, which affects the rate at which action potentials are triggered in sensory neurons. Notably, both excessively high and low lipophilicity can reduce activation kinetics, leading to a slower rate of action potential initiation in sensory neurons and consequently lower pungency.

Based on this, we expected that COOH-CAP (Log$P$ = 3.31; Fig. 2A) would have reduced irritancy compared to capsaicin (Log$P$ = 3.66) due to its less lipophilic nature. To confirm this, we compared the irritancy of capsaicin and COOH-CAP using a rat behavioral assay. A 10 μL solution containing 0.11 μmol of either compound (with 0.25 mg Tween 20), or PBS, was injected into the hindpaw of rats ($n = 6$). The frequency and duration of the rats' paw licking were then observed and recorded. As expected, after injecting the 1 × PBS solution, there was no foot-licking behavior. After injecting the COOH-CAP prodrug, the average frequency of foot licking was 0.5 ± 1.0 times, and the average duration was 2.2 ± 4.3 s (Fig. 9A and B). In comparison, rats injected with the same dose of plain capsaicin exhibited an

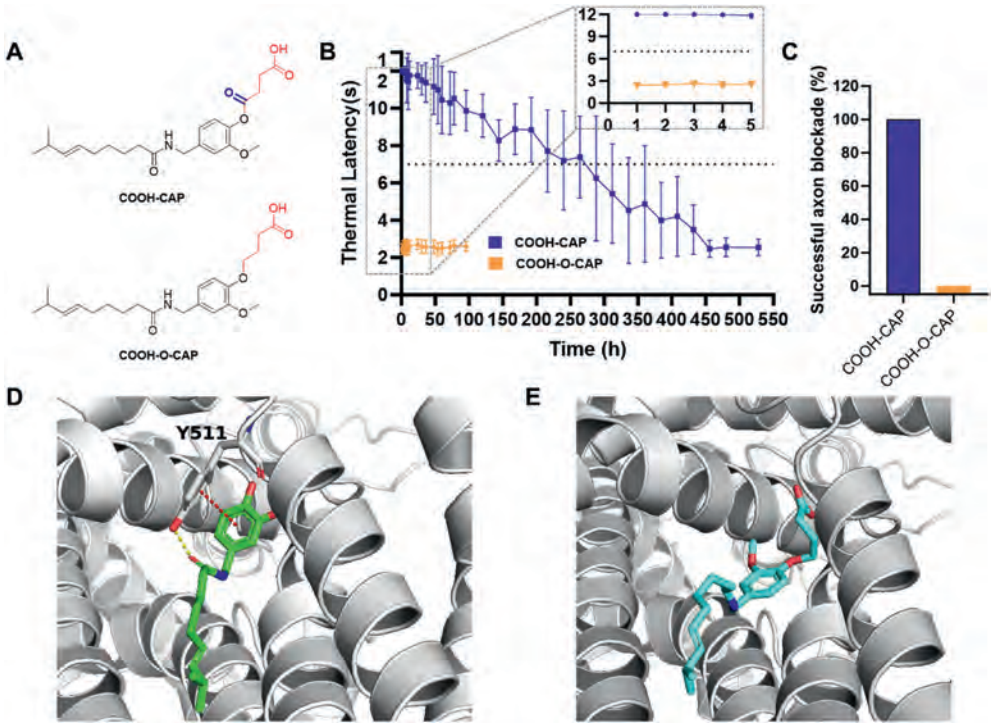

Figure 8 Assessment of the nerve-blocking efficacy of the prodrug itself. (A) Structures of the COOH-CAP and COOH-*O*-CAP prodrugs. (B) Comparison of ipsilateral thermal latencies in rats' post-administration with 3.28 μmol COOH-CAP and 3.28 μmol COOH-*O*-CAP prodrug. $n = 6$. Data are expressed as mean ± SD. (C) Percentage of rats with successful axon blockade. (D) Published binding mode of capsaicin with TRPV1 (generated from PDB code 7LPE). The atoms of capsaicin are colored as follows: carbon, green; oxygen, red; nitrogen, blue. The cartoon shows the protein and key residues are colored as follows: carbon, grey; oxygen, red; nitrogen, blue. Yellow dotted lines indicate H-bonds, and the red dotted lines represent $\pi-\pi$ stacking interactions. (E) Proposed binding mode of COOH-*O*-CAP with TRPV1. The atoms of COOH-*O*-CAP are colored as follows: carbon, blue; oxygen, red; nitrogen, blue.

average frequency of 6.3 ± 2.8 times and an average duration of 24.5 ± 5.9 s.

It has been well established in previous studies that intraplantar injection of capsaicin or its analogs reduces mechanical withdrawal thresholds, reflecting enhanced mechanical sensitivity[67]. Consistent with this, mechanical hypersensitivity tests in rats, assessed using the von Frey up-down method[68] showed that intraplantar injection of 10 μL of 1 × PBS solution containing either 0.11 μmol of COOH-CAP, 0.11 μmol of CAP, or PBS alone induced different levels of mechanical sensitivity. The injection of COOH-CAP induced mild sensitivity, with the threshold returning to baseline by 45 min (Fig. 9C). In contrast, the injection of capsaicin induced a significant and prolonged decrease in the 50% withdrawal threshold, which recovered after 150 min. These results are consistent with the findings from the paw licking assay, further supporting that COOH-CAP induces significantly less sensory irritation compared to capsaicin.

In addition to its lower lipophilicity, the reduced irritancy of COOH-CAP may also be attributed to its slow-release behavior, which leads to a lower effective concentration of free capsaicin at the site of injection over time, thereby avoiding acute spikes in local capsaicin concentration that typically cause strong sensory irritation.

This reduction in irritancy does not compromise nerve block efficacy, as TRPV1-mediated irritation and nerve block arise through distinct mechanisms. These two effects also occur at different stages of TRPV1 activation. Acute irritation results from rapid TRPV1 activation on nociceptive neurons, which induces immediate depolarization and action potential firing. This irritation is confined to the early phase of activation—from initial receptor binding to peak TRPV1 opening. Compounds with excessively high or low lipophilicity tend to exhibit faster receptor activation kinetics, thereby efficiently triggering neuronal excitation and the release of neuropeptides such as substance P and CGRP. This cascade underlies the observed pungency and pain response following TRPV1 agonist administration[66]. The prolonged nerve block is mediated by downstream effects such as calcium overload, mitochondrial dysfunction, and neuropeptide depletion. These effects emerge after the initial activation phase and represent the later intracellular response stage. These cellular events lead to defunctionalization—a prolonged loss of sensory function in peripheral TRPV1-expressing nociceptive terminals[63,69]. This mechanistic dissociation explains why brief irritation can coexist with sustained analgesia, as exemplified by the 8% capsaicin patch, which causes short-term burning yet provides pain relief for weeks[64]. Similarly, COOH-CAP induces only mild, short-lived irritation while achieving long-lasting nerve blockade.

3. Discussion

The prolonged duration of capsaicin-induced nerve block highlights a fundamental difference between TRPV1-targeting agents and conventional local anesthetics. Unlike sodium channel blockers

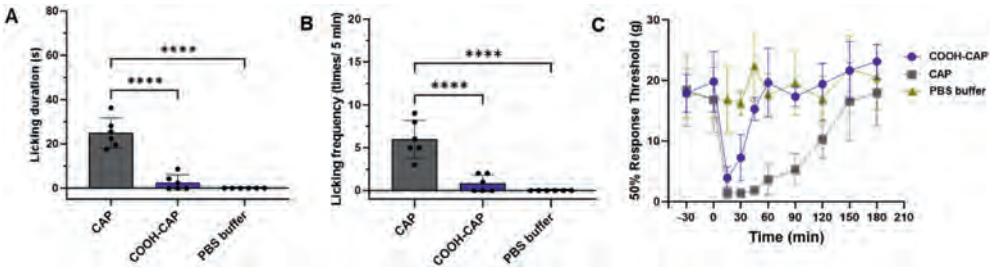

Figure 9 Evaluation of the irritancy of capsaicin in the hindpaw of rats. Licking frequency (A) and licking duration (B) during the first 5 min after intraplantar injection of 10 μL of 1 × PBS solution containing 0.11 μmol of COOH-CAP, 0.25 mg of Tween 20, 0.11 μmol of CAP and 0.25 mg of Tween 20, or a 1 × PBS solution in the hindpaw of rats. (C) Mechanical sensitivity assessed using the von Frey up-down method following intraplantar injection of the same formulations. Data are presented as mean ± SD ($n = 6$). One-way ANOVA followed by Tukey's test; ****$P < 0.0001$.

such as bupivacaine, which require continuous presence at the nerve site to maintain efficacy, capsaicin produces long-lasting nerve block even after the drug is cleared from the tissue. Capsaicin-induced nerve block persists far beyond its pharmacokinetic half-life and does not rely on sustained receptor occupancy[63,69]. This prolonged effect is mediated by the process of defunctionalization, in which TRPV1-positive nociceptive neurons undergo functional silencing following intense or sustained activation.

Upon binding to TRPV1, capsaicin triggers a sustained calcium influx into nociceptive neurons, initiating a cascade of intracellular events including mitochondrial dysfunction, cytoskeletal collapse, and neuropeptide depletion (*e.g.*, substance P). These changes disrupt the ability of nociceptive terminals to propagate action potentials, thereby leading to a long-lasting loss of sensory function. Importantly, this effect is independent of the drug's residence time in local tissue. For instance, the 8% high-concentration capsaicin patch has a reported subcutaneous half-life of only 1.64 h, yet it can produce pain relief lasting for several weeks[64].

This mechanistic distinction is reflected in their markedly different durations of action. In our previous studies, a single injection of 1 mg capsaicin into the sciatic nerve produced a sensory block lasting approximately 6.8 h[49], whereas 1.5 mg of bupivacaine administered *via* the same route produced a much shorter block of only 1.7 h[56]. These results emphasize that the efficacy of capsaicin is not governed by its pharmacokinetics but by the irreversible or slowly reversible effects it induces at the cellular level.

Based on this understanding, we propose that the prolonged duration of action observed with COOH-CAP arises not only from the slow conversion of the COOH-CAP prodrug to capsaicin, but also from the downstream defunctionalization of nociceptive neurons. In addition, its ability to penetrate the perineurium *via* MCT1 transport further contributes to the extended duration of nerve block.

4. Conclusions

We have shown that functionalizing nerve-blocking agents with a carboxyl group through hydrolysable ester bond is an effective method for enhancing their effectiveness in nerve block and reducing their side effects. The carboxyl group utilizes the MCT1-mediated transport mechanism to enhance drug transport across the PNBs and permeation into the endoneurium. This leads to an increased bioavailability of nerve-blocking agents to peripheral nerve axons. Additionally, the slow hydrolysis of ester bond achieves a sustained release of the active drug. This helps maintain effective and safe drug concentration for an extended period. COOH-CAP was confirmed to activate TRPV1 in human HEK293 cells expressing TRPV1, with an EC_{50} of 2.96 nmol/L in calcium flux assays and 449 nmol/L in patch-clamp recordings, which is comparable to that of capsaicin. In addition, *in vivo* thermoregulation studies demonstrated that COOH-CAP induced transient hypothermia through TRPV1 activation, which could be reversed by the TRPV1 antagonist AMG9810, further confirming a TRPV1-mediated mechanism. In rat studies, the injection of COOH-CAP prodrug around the sciatic nerve resulted in a significantly longer duration of nerve block compared to an equivalent dose of plain capsaicin. Notably, a single injection of 3.28 μmol of the COOH-CAP prodrug in a rat sciatic nerve model led to a sensory nerve blockade lasting 260.0 ± 83.7 h, without causing significant motor impairment or any capsaicin-related side effects or toxicity. Even at a lower dose (1.64 μmol), COOH-CAP prodrug still produced a sensory nerve blockade lasting 172.0 ± 41.3 h. The enhanced permeability of the nerve-blocking agents will allow for smaller doses of drugs and prolong the effect. Using smaller doses has many benefits, including better safety in case of an intravascular injection and the ability to block several nerves without the fear of overdose.

5. Experimental

5.1. Materials

All chemicals and solvents were purchased at the highest purity available on the market. Natural capsaicin (capsaicin: dihydrocapsaicin ratio of approximately 3:1), succinylated derivatives, potassium carbonate, pyridine, valeryl chloride, valeryl chloride, and triethylamine were supplied by Sigma−Aldrich (St. Louis, MO, USA). DMAP, silica gels, PBS buffer (pH 7.4), FITC, 5-FAM, 5-AFM, CHC and other organic solvents were purchased from VWR International Ltd (Radnor, PA, USA). High-resolution mass spectrumetry (HRMS) was acquired using a Waters ESI-TOF high-resolution mass spectrometer. Proton nuclear magnetic resonance (^{1}H NMR) spectra were recorded at 500 MHz, while carbon-13 nuclear magnetic resonance (^{13}C NMR) spectra were recorded at 101 MHz. Chemical shifts were expressed in delta (δ) units in parts per million (ppm), with the δ 0 signal from tetramethylsilane and the δ 7.26 signal from CDCl3 serving as internal standards.

5.2. Synthesis and characterization

Experimental details of the synthetic works were included in the Supporting Information

5.3. Measurement of chemical stability and metabolic degradation

To evaluate the chemical stability of COOH-CAP, 5 mg of the compound was dissolved in 10 mL of Milli-Q water and incubated at 37 °C on a heating block. At predetermined time points (1, 2.5, 3.5, 4.5, 5.5, 6.5, 8.5, 10.5, 12.5, 24.5, and 26.5 h), 80 μL aliquots were collected and directly analyzed using a UPLC system (Waters, Milford, MA, USA).

For the metabolic degradation study, fresh rat sciatic nerves (∼1 cm segments) were homogenized in 1 mL of ice-cold 1 × PBS using a glass tissue grinder. COOH-CAP (5 mg) was added to the homogenate, and the mixture was incubated at 37 °C. At designated time points (30, 45, 60, 75, and 90 min), 200 μL aliquots were withdrawn and immediately quenched with an equal volume of ice-cold acetonitrile. The samples were centrifuged at 14,000 rpm (Eppendorf 5810R Refrigerated Centrifuge, CT, USA) for 10 min, and the resulting supernatants were analyzed by high-resolution mass spectrometry (HRMS) to quantify the remaining parent compound.

5.4. Calcium flux assay and patch-clamp electrophysiology

A calcium flux assay was conducted by Creative Biolabs (Shirley, NY, USA), a contract research organization, using HEK293 cells stably expressing the human TRPV1 receptor (hTRPV1). Cells were seeded into 384-well plates at a density of 1.2×10^4 cells per well in 25 μL of culture medium and incubated for 16−20 h at 37 °C in a humidified atmosphere with 5% CO_2.

On the following day, the assay was performed using the FLIPR Calcium 6 Assay Kit. The culture medium was removed, and each well was loaded with 40 μL of 1 × dye loading buffer. Plates were incubated in the dark at 37 °C for 2 h. Test compounds were diluted in DMSO and transferred to the assay plate *via* acoustic dispensing (100 nL/well), followed by the addition of 20 μL of assay buffer. Compounds were tested in triplicate using a 10-point, 3-fold serial dilution starting from 10 μmol/L. Capsaicin (positive control) and 0.1% DMSO (vehicle control) were included in parallel.

After the addition of 10 μL compound solution to each well, fluorescence signals were measured in real-time over 5 min using a FLIPR instrument (excitation: 470−515 nm, emission: 515−575 nm). Data were processed in GraphPad Prism using nonlinear regression to generate dose-response curves and calculate EC_{50} values. Assay performance was evaluated by calculating signal-to-background ratio (S/B), coefficient of variation (CV), and Z′-factor.

Whole-cell patch-clamp recordings were conducted By Sciline (Beijing, China), a contract research organization, on HEK293 cells stably expressing TRPV1. Cells were seeded onto glass coverslips and used after adherence. The extracellular solution contained (in mmol/L): 137 NaCl, 1 $MgCl_2$, 4 KCl, 10 glucose, and 10 HEPES (pH 7.4). The intracellular pipette solution contained (in mmol/L): 50 CsCl, 60 CsF, 10 HEPES, 20 EGTA, and 10 NaCl (pH 7.2).

Recordings were performed using an EPC-10 amplifier and PatchMaster software. Cells were voltage-clamped at −80 mV, and a ramp from −120 to +120 mV over 200 ms was applied every 10 s. COOH-CAP was applied cumulatively at increasing concentrations (1 nmol/L to 30 μmol/L), and inward currents were recorded. Data were analyzed by normalizing peak current responses relative to baseline and maximum response.

5.5. Animal studies

The animal experiments were conducted in accordance with a protocol approved by the University of Alabama's Institutional Animal Care and Use Committee (Protocol Number: 19-11-2992). This study utilized adult male Sprague-Dawley rats, each weighing between 250 and 350 g, which were acquired from Charles River Laboratories in Wilmington, Massachusetts, USA. The rats were kept in pairs within each cage under a 12-h light/dark cycle. Prior to drug administration, the rats were briefly anesthetized with isoflurane delivered *via* a face mask. The drug formulations, including COOH-CAP, AMG9810, Valeryl-CAP, COOH-CAP@CHC, and COO-O-CAP, were initially dissolved in methanol containing a Tween 20 solution. Afterward, the solvent was removed through vacuum evaporation. These formulations were then re-dissolved in 0.1 or 0.3 mL of 1 × PBS buffer to achieve the desired drug concentrations and were thoroughly mixed with 7.5 mg of Tween 20 using a vortex mixer before injection.

For the thermal responsiveness study, injections were administered into the left leg of each rat using a 23 G × 3/4″ needle inserted from the posterior medial aspect of the greater trochanter, directing the needle anteriorly and medially. Upon contacting the bone, 0.3 mL of the formulation was injected. Neurological assessments were performed at defined time points post-injection in a single-blinded manner. The right leg served as a control to assess potential systemic effects.

Thermal latency, defined as the duration the rats could endure placing their hind paw on a heated plate set at 56 °C (Model 39D Hot Plate Analgesia Meter, IITC Inc., Woodland Hills, CA, USA), was measured. To prevent injury, the paw was removed after 12 s. Each time point was tested three times, and the average result was calculated. Motor function was evaluated by measuring the extensor postural thrust, which recorded the maximum weight a hind paw could support without the ankle touching the scale.

The duration of sensory blockade was determined by the time it took for thermal latency to return to 7 s, considering the baseline thermal latency was approximately 2 s, with 7 s representing the midpoint between the maximum latency of 12 s and the baseline. The duration of the motor blockade was defined by the time required for the weight-bearing capacity to return to 50% of its initial value (additional experimental details are provided in the Supporting Information).

For the thermoregulation study, core body temperature was monitored in adult rats after intraperitoneal injection of the test compounds (*e.g.*, COOH-CAP or capsaicin). On the day of the experiment, rats received an intraperitoneal injection of the compound at an equivalent molar dose dissolved in 100 μL of 1 × PBS containing 0.25 mg of Tween 20. Baseline core temperature was recorded using a digital rectal thermometer (PTM1 Portable Temperature Monitor, Physitemp Instruments, Clifton, NJ, USA) prior to injection, and subsequent measurements were taken at defined time points (*e.g.*, 15, 30, 45, 60, 90, 120, 150, and 180 min post-injection). To verify TRPV1-mediated effects, a TRPV1 antagonist (AMG9810, 5 mg) was intraperitoneally administered 30 min prior to the injection of the test compound in selected animals. Core body temperatures were recorded at defined time points, and temperature changes over time were compared between groups with or without AMG9810 pretreatment to confirm the TRPV1 dependency of the hypothermic responses induced by the compounds.

5.6. Molecular docking

Import the protein PDB file into AutoDock Tools, add hydrogens, and save it as a PDBQT file. Next, load the small molecule file in MOL2 format, verify its structure, adjust torsional bonds as necessary, and save it as a PDBQT file. After preparing both the receptor and ligand files, load them into AutoDock Tools, define the docking box parameters, and save the configuration file. Place vina.exe, the configuration file, and the receptor and ligand files in the same directory. Execute AutoDock Vina to perform the docking process. The output will automatically display binding energies ranked from lowest to highest. Select the conformation with the lowest binding energy and create the complex with the protein. Finally, use PyMOL 3.1 for visualization and detailed analysis of the results.

5.7. In vivo distribution of FITC, 5-AFM, 5-FAM, and 5-FAM@CHC

While under anesthesia with isoflurane and oxygen, a 0.3 mL test solution containing FITC, 5-AFM, 5-FAM, or 5-FAM@CHC in PBS buffer was injected near the sciatic nerve. The injections were carefully administered to ensure each compound was delivered at an equal molar concentration. After a 4-h interval, the sciatic nerves were harvested and embedded in OCT compound for the preparation of frozen sections. A coverslip was then applied to the sections, which were subsequently imaged using a Leica TCS SP2 confocal microscope.

To evaluate the depth of penetration of the injected compounds within the nerve, a quantitative analysis of the confocal fluorescence images was performed. The nerve was segmented into 10 equally spaced concentric zones based on its morphology, and the fluorescence intensities across these zones were quantified using ImageJ software.

5.8. Tissue harvesting and histology

If continuous sensory blockade was not evident, rats were euthanized either 14 or 28 days after the injection. The sciatic nerve, along with surrounding tissues, was harvested to evaluate potential chronic inflammation and nerve degeneration. Muscle tissues were preserved in 10% neutral buffered formalin and prepared for histological analysis using standard techniques. Hematoxylin and eosin staining was performed on the slides, after which the muscle tissues were scored for inflammation on a 0−4 scale and myotoxicity on a 0−6 scale[60]. Histological evaluations of inflammation and myotoxicity were conducted in a single-blinded manner. Inflammation severity was assessed subjectively based on the extent of immune cell infiltration. Myotoxicity was evaluated according to two hallmark features of local anesthetic-induced damage: nuclear internalization and muscle fiber regeneration. Nuclear internalization was defined as the presence of centrally located nuclei within otherwise normal-appearing myocytes, deviating from their typical peripheral position[70]. Regenerating fibers were identified by their reduced size and basophilic cytoplasm, indicative of active tissue repair[49,56,58,71]. The scoring system was as follows: 0 = normal; 1 = perifascicular internalization; 2 = deep internalization (>5 cell layers); 3 = perifascicular regeneration; 4 = deep regeneration; 5 = hemifascicular regeneration; 6 = holofascicular regeneration.

To evaluate neurotoxicity, the sciatic nerve samples were fixed in Karnovsky's KII Solution (comprising 2.5% glutaraldehyde, 2.0% paraformaldehyde, and 0.025% calcium chloride in 0.1 mol/L cacodylate buffer, pH 7.4). Post-fixation was carried out with osmium tetroxide for 2 h, followed by dehydration in a graded series of ethanol concentrations (30%, 60%, 90%, 100%, 100%, and 100%) for 10 min each. The dehydrated nerves were then infiltrated with a mixture of ethanol and Epon resin at ratios of 1:1, 1:2, and finally pure resin. The nerves were sectioned using a diamond knife on an ultramicrotome, producing 800 nm sections, which were stained with toluidine blue for light microscopy. Additionally, 100 nm sections were examined under a transmission electron microscope (TEM, Hitachi H-7650), and nerve diameters were measured using ImageJ software.

5.9. Evaluation of irritancy and mechanical hypersensitivity

Male rats ($n = 6$ per group) received a single intraplantar injection (10 μL) into the hindpaw of either COOH-CAP (0.11 μmol, with 0.25 mg Tween 20), capsaicin (0.11 μmol, with 0.25 mg Tween 20), or 1 × PBS as a control. Immediately following the injection, paw-licking behavior was monitored for 5 min to assess acute irritancy, with both licking frequency and duration recorded.

Mechanical sensitivity was assessed using the von Frey up-down method at designated time points (0 to 210 min post-injection)[68]. A set of calibrated von Frey filaments was applied perpendicularly to the plantar surface of the injected hindpaw until slight bending occurred. Each trial was recorded as a positive (X, withdrawal) or negative (O, no withdrawal) response. Testing continued until the first change in response pattern (*e.g.*, from X to O or O to X) was observed. Starting from the response immediately before this change, a total of six consecutive responses—including the change point and four subsequent trials—were recorded. The 50% paw withdrawal threshold was calculated using Dixon's up-down method based on these six responses.

Acknowledgments

Research reported in this publication was supported by the National Institute of General Medical Sciences of the National Institutes of Health (Award No. R01GM144388, USA) and by the National Institute of Neurological Disorders and Stroke of the National Institutes of Health (Award Nos: R61NS123196 and R33NS123196, USA).

Author contributions

Yu Wen, Tian Yang, Qi Li, Xiaosi Li, Xiaoyan Ma, Huiyang Hu, Prabhakar Busa, Sayma Alamb, and Chao Zhao planned and carried out the experiments and analyzed the data. Yu Wen and Chao Zhao wrote the paper. Libo Tan and Xiaosi Li provided intellectual input and contributed to editing the final manuscript. Chao Zhao conceived the presented idea. Chao Zhao supervised the project. Yu Wen and Tian Yang contributed equally to this work.

Conflicts of interest

The authors declare no conflicts of interest.

Appendix A. Supporting information

Supporting information to this article can be found online at https://doi.org/10.1016/j.apsb.2025.11.006.

References

1. Worldwide Surgical Procedure Volumes Growing through 2023 with Accelerated Growth in Key Segments. 2019. Available from: https://www.lifesciencemarketresearch.com/insights/worldwide-surgical-procedure-volumes-growing-through-2023-with-accelerated-growth-in-key-segments.
2. Coppes OJM, Yong RJ, Kaye AD, Urman RD. Patient and surgery-related predictors of acute postoperative pain. *Curr Pain Headache Rep* 2020;**24**:12.
3. Vidal-Torres A, Fernández-Pastor B, García M, Ayet E, Cabot A, Burgueno J, et al. Bispecific sigma-1 receptor antagonism and mu-opioid receptor partial agonism: WLB-73502, an analgesic with improved efficacy and safety profile compared to strong opioids. *Acta Pharm Sin B* 2023;**13**:82−99.
4. Vinyes D, Muñoz-Sellart M, Fischer L. Therapeutic use of low-dose local anesthetics in pain, inflammation, and other clinical conditions: a systematic scoping review. *J Clin Med* 2023;**12**:7221.
5. Becker DE, Reed KL. Local anesthetics: review of pharmacological considerations. *Anesth Prog* 2012;**59**:90−102.
6. Joshi G, Gandhi K, Shah N, Gadsden J, Corman SL. Peripheral nerve blocks in the management of postoperative pain: challenges and opportunities. *J Clin Anesth* 2016;**35**:524−9.
7. Berde CB, Athiraman U, Yahalom B, Zurakowski D, Corfas G, Bognet C. Tetrodotoxin-bupivacaine-epinephrine combinations for prolonged local anesthesia. *Mar Drugs* 2011;**9**:2717−28.
8. Dinges HC, Wiesmann T, Otremba B, Wulf H, Eberhart LH, Schubert AK. The analgesic efficacy of liposomal bupivacaine compared with bupivacaine hydrochloride for the prevention of postoperative pain: a systematic review and meta-analysis with trial sequential analysis. *Reg Anesth Pain Med* 2021;**46**:490−8.
9. Ilfeld BM, Eisenach JC, Gabriel RA. Clinical effectiveness of liposomal bupivacaine administered by infiltration or peripheral nerve block to treat postoperative pain. *Anesthesiology* 2021;**134**:283−344.
10. Orebaugh SL, Dewasurendra A. Has the future arrived? Liposomal bupivacaine *versus* perineural catheters and additives for interscalene brachial plexus block. *Curr Opin Anaesthesiol* 2020;**33**:704−9.
11. Wang Z, Huang H, Yang S, Huang S, Guo J, Tang Q, et al. Long-term effect of ropivacaine nanoparticles for sciatic nerve block on postoperative pain in rats. *Int J Nanomed* 2016;**11**:2081−90.
12. Leasia K, Ciarallo C, Prins JTH, Preslaski C, Perkins-Pride E, Hardin K, et al. A randomized clinical trial of single dose liposomal bupivacaine *versus* indwelling analgesic catheter in patients undergoing surgical stabilization of rib fractures. *J Trauma Acute Care Surg* 2021;**91**:872−8.
13. Padera R, Bellas E, Tse JY, Hao D, Kohane DS. Local myotoxicity from sustained release of bupivacaine from microparticles. *Anesthesiology* 2008;**108**:921−8.
14. Pere P, Watanabe H, Pitkänen M, Wahlström T, Rosenberg PH. Local myotoxicity of bupivacaine in rabbits after continuous supraclavicular brachial plexus block. *Reg Anesth* 1993;**18**:304−7.
15. Chard PS, Bleakman D, Savidge JR, Miller RJ. Capsaicin-induced neurotoxicity in cultured dorsal root ganglion neurons: involvement of calcium-activated proteases. *Neuroscience* 1995;**65**:1099−108.
16. Gabriel RA, Ilfeld BM. Peripheral nerve blocks for postoperative analgesia: from traditional unencapsulated local anesthetic to liposomes, cryoneurolysis and peripheral nerve stimulation. *Best Pract Res Clin Anaesthesiol* 2019;**33**:293−302.
17. Lirk P, Hollmann MW, Strichartz G. The science of local anesthesia: basic research, clinical application, and future directions. *Anesth Analg* 2018;**126**:1381−92.
18. Sun Y, Zabihi M, Li Q, Li X, Kim BJ, Ubogu EE, et al. Drug permeability: from the blood−brain barrier to the peripheral nerve barriers. *Adv Ther* 2023;**6**:2200150.
19. Borthakur A, Saksena S, Gill RK, Alrefai WA, Ramaswamy K, Dudeja PK. Regulation of monocarboxylate transporter 1 (MCT1) promoter by butyrate in human intestinal epithelial cells: involvement of NF-κB pathway. *J Cell Biochem* 2008;**103**:1452−63.
20. Halestrap AP, Meredith D. The SLC16 gene family−from monocarboxylate transporters (MCTs) to aromatic amino acid transporters and beyond. *Pflügers Archiv* 2004;**447**:619−28.
21. Wang Y, Tonouchi M, Miskovic D, Hatta H, Bonen A. T3 increases lactate transport and the expression of MCT4, but not MCT1, in rat skeletal muscle. *Am J Physiol Endocrinol Metab* 2003;**285**:E622−8.
22. Halestrap AP, Price NT. The proton-linked monocarboxylate transporter (MCT) family: structure, function and regulation. *Biochem J* 1999;**343**:281−99.
23. Meredith D, Christian H. The SLC16 monocaboxylate transporter family. *Xenobiotica* 2008;**38**:1072−106.
24. Fischer K, Hoffmann P, Voelkl S, Meidenbauer N, Ammer J, Edinger M, et al. Inhibitory effect of tumor cell−derived lactic acid on human T cells. *Blood* 2007;**109**:3812−9.
25. Kang Y, Terasaki T, Tsuji A. Acidic drug transport *in vivo* through the blood−brain barrier. A role of the transport carrier for monocarboxylic acids. *J Pharmacobio-Dyn* 1990;**13**:158−63.
26. Li G, Shao K, Umeshappa CS. Recent progress in blood−brain barrier transportation research. *Brain Target Drug Deliv Syst* 2019:33−51.
27. Vijay N, Morris ME. Role of monocarboxylate transporters in drug delivery to the brain. *Curr Pharm Des* 2014;**20**:1487−98.
28. Rawat A, Morrison BM. Metabolic transporters in the peripheral nerve−what, where, and why?. *Neurotherapeutics* 2021;**18**:2185−99.
29. Morrison BM, Tsingalia A, Vidensky S, Lee Y, Jin L, Farah MH, et al. Deficiency in monocarboxylate transporter 1 (MCT1) in mice delays regeneration of peripheral nerves following sciatic nerve crush. *Exp Neurol* 2015;**263**:325−38.
30. Jha MK, Ament XH, Yang F, Liu Y, Polydefkis MJ, Pellerin L, et al. Reducing monocarboxylate transporter MCT1 worsens experimental diabetic peripheral neuropathy. *Exp Neurol* 2020;**333**:113415.
31. Morrison B, Tsingalia A, Lengacher S, Pellerin L, Magistretti P, Rothstein J. Monocarboxylate transporter 1 (Mct1) is critical for regeneration in peripheral nerves. *J Peripher Nerv Syst* 2013;**18**:74.
32. Sun L, Zhang J, Niu C, Deering-Rice CE, Hughen RW, Lamb JG, et al. CYP1B1-derived epoxides modulate the TRPA1 channel in chronic pain. *Acta Pharm Sin B* 2023;**13**:68−81.
33. Caterina MJ, Schumacher MA, Tominaga M, Rosen TA, Levine JD, Julius D. The capsaicin receptor: a heat-activated ion channel in the pain pathway. *Nature* 1997;**389**:816−24.
34. Zhong T, Zhang W, Guo H, Pan X, Chen X, He Q, et al. The regulatory and modulatory roles of TRP family channels in malignant tumors and relevant therapeutic strategies. *Acta Pharm Sin B* 2022;**12**:1761−80.
35. Dawson-Basoa ME, Gintzler AR. Estrogen and progesterone activate spinal kappa-opiate receptor analgesic mechanisms. *Pain* 1996;**64**:169−77.
36. Caterina MJ, Julius D. The vanilloid receptor: a molecular gateway to the pain pathway. *Annu Rev Neurosci* 2001;**24**:487−517.
37. Jancśo G, Király E, Jancsó-Gábor A. Direct evidence for an axonal site of action of capsaicin. *Naunyn-Schmiedebergs Arch Pharmacol* 1980;**313**:91−4.
38. Knotkova H, Pappagallo M, Szallasi A. Capsaicin (TRPV1 agonist) therapy for pain relief: farewell or revival?. *Clin J Pain* 2008;**24**:142−54.
39. Oszlács O, Jancsó G, Kis G, Dux M, Sántha P. Perineural capsaicin induces the uptake and transganglionic transport of choleratoxin B subunit by nociceptive C-fiber primary afferent neurons. *Neuroscience* 2015;**311**:243−52.
40. Jancso G, Lynn B. Possible use of capsaicin in pain therapy. *Clin J Pain* 1987;**3**:123−6.

41. Fitzgerald M, Woolf C. The time course and specificity of the changes in the behavioural and dorsal horn cell responses to noxious stimuli following peripheral nerve capsaicin treatment in the rat. *Neuroscience* 1982;**7**:2051−6.
42. Jancsó G, Lawson S. Transganglionic degeneration of capsaicin-sensitive C-fiber primary afferent terminals. *Neuroscience* 1990;**39**: 501−11.
43. Pini A, Lynn B. C-fibre function during the 6 weeks following brief application of capsaicin to a cutaneous nerve in the rat. *Eur J Neurosci* 1991;**3**:274−84.
44. Kissin I. Vanilloid-induced conduction analgesia: Selective, dose-dependent, long-lasting, with a low level of potential neurotoxicity. *Anesth Analg* 2008;**107**:271−81.
45. Jancsó G, Dux M, Oszlács O, Sántha P. Activation of the transient receptor potential vanilloid-1 (TRPV1) channel opens the gate for pain relief. *Br J Pharmacol* 2008;**155**:1139−41.
46. Chard P, Bleakman D, Savidge J, Miller R. Capsaicin-induced neurotoxicity in cultured dorsal root ganglion neurons: involvement of calcium-activated proteases. *Neuroscience* 1995;**65**:1099−108.
47. Ilie MA, Caruntu C, Tampa M, Georgescu SR, Matei C, Negrei C, et al. Capsaicin: physicochemical properties, cutaneous reactions and potential applications in painful and inflammatory conditions. *Exp Ther Med* 2019;**18**:916−25.
48. Liu Q, Santamaria CM, Wei T, Zhao C, Ji T, Yang T, et al. Hollow silica nanoparticles penetrate the peripheral nerve and enhance the nerve blockade from tetrodotoxin. *Nano Lett* 2018;**18**:32−7.
49. Li Q, Li X, Zhang Y, Yang Q, Hathcock SF, Cai Y, et al. Galacturonic acid-capsaicin prodrug for prolonged nociceptive-selective nerve blockade. *J Control Release* 2024;**371**:324−37.
50. Carozzi VA, Canta A, Oggioni N, Ceresa C, Marmiroli P, Konvalinka J, et al. Expression and distribution of 'high affinity' glutamate transporters GLT1, GLAST, EAAC1 and of GCPII in the rat peripheral nervous system. *J Anat* 2008;**213**:539−46.
51. Yang S, Fan W, Xu Y. Melanoidins from Chinese distilled spent grain: content, preliminary structure, antioxidant, and ACE-inhibitory activities *in vitro*. *Foods* 2019;**8**:516.
52. Song H, Lee SY. Production of succinic acid by bacterial fermentation. *Enzym Microb Technol* 2006;**39**:352−61.
53. Zeikus J, Jain M, Elankovan P. Biotechnology of succinic acid production and markets for derived industrial products. *Appl Microbiol Biotechnol* 1999;**51**:545−52.
54. Liang Q, Qiao Z, Zhou Q, Xue D, Wang K, Shao L. Discovery of potent and selective transient receptor potential vanilloid 1 (TRPV1) agonists with analgesic effects *in vivo* based on the functional conversion induced by altering the orientation of the indazole core. *J Med Chem* 2022;**65**:11658−78.
55. Romeo I, Brizzi A, Pessina F, Ambrosio FA, Aiello F, Belardo C, et al. *In silico*-guided rational drug design and synthesis of novel 4-(thiophen-2-yl) butanamides as potent and selective TRPV1 agonists. *J Med Chem* 2023;**66**:6994−7015.
56. Ji T, Li Y, Deng X, Rwei AY, Offen A, Hall S, et al. Delivery of local anaesthetics by a self-assembled supramolecular system mimicking their interactions with a sodium channel. *Nat Biomed Eng* 2021;**5**:1099−109.
57. Cai Y, Li Q, Wesselmann U, Zhao C. Exosomal bupivacaine: integrating nerve barrier penetration capability and sustained drug release for enhanced potency in peripheral nerve block and reduced toxicity. *Adv Funct Mater* 2024;**34**:2406876.
58. Ma X, Cai Y, Gurung SK, Rao SS, Zhao C. Glucose-facilitated nanomicelles cross peripheral nerve barriers to achieve drug delivery to nerves. *Adv Funct Mater* 2025;**35**:2423036.
59. Hoppe K, Sznitowska M. The effect of polysorbate 20 on solubility and stability of candesartan cilexetil in dissolution media. *AAPS PharmSciTech* 2014;**15**:1116−25.
60. McAlvin JB, Padera RF, Shankarappa SA, Reznor G, Kwon AH, Chiang HH, et al. Multivesicular liposomal bupivacaine at the sciatic nerve. *Biomaterials* 2014;**35**:4557−64.
61. Fischer MJ, Ciotu CI, Szallasi A. The mysteries of capsaicin-sensitive afferents. *Front Physiol* 2020;**11**:554195.
62. Kwon D, Zhang F, Suo Y, Bouvette J, Borgnia MJ, Lee SY. Heat-dependent opening of TRPV1 in the presence of capsaicin. *Nat Struct Mol Biol* 2021;**28**:554−63.
63. Anand P, Bley K. Topical capsaicin for pain management: therapeutic potential and mechanisms of action of the new high-concentration capsaicin 8% patch. *Br J Anaesth* 2011;**107**:490−502.
64. O'Neill J, Brock C, Olesen AE, Andresen T, Nilsson M, Dickenson AH. Unravelling the mystery of capsaicin: a tool to understand and treat pain. *Pharmacol Rev* 2012;**64**:939−71.
65. Szallasi A, Blumberg PM. Vanilloid (Capsaicin) receptors and mechanisms. *Pharmacol Rev* 1999;**51**:159−212.
66. Ursu D, Knopp K, Beattie RE, Liu B, Sher E. Pungency of TRPV1 agonists is directly correlated with kinetics of receptor activation and lipophilicity. *Eur J Pharmacol* 2010;**641**:114−22.
67. Binshtok AM, Bean BP, Woolf CJ. Inhibition of nociceptors by TRPV1-mediated entry of impermeant sodium channel blockers. *Nature* 2007;**449**:607−10.
68. Chaplan SR, Bach FW, Pogrel J, Chung J, Yaksh T. Quantitative assessment of tactile allodynia in the rat paw. *J Neurosci Methods* 1994;**53**:55−63.
69. Chung MK, Campbell JN. Use of capsaicin to treat pain: mechanistic and therapeutic considerations. *Pharmaceuticals* 2016;**9**:66.
70. Padera R, Bellas E, Julie YT, Hao D, Kohane DS. Local myotoxicity from sustained release of bupivacaine from microparticles. *Anesthesiology* 2008;**108**:921.
71. Zink W, Bohl JRE, Hacke N, Sinner B, Martin E, Graf BM. The long term myotoxic effects of bupivacaine and ropivacaine after continuous peripheral nerve blocks. *Anesth Analg* 2005;**101**: 548−54.
72. Ohtsu N, Ohgaki R, Jin C, Xu M, Okanishi H, Takahashi R, et al. Functional coupling of organic anion transporter OAT10 (SLC22A13) and monocarboxylate transporter MCT1 (SLC16A1) influencing the transport function of OAT10. *J Pharmacol Sci* 2022; **150**:41−8.
73. Ahlin G, Hilgendorf C, Karlsson J, Szigyarto CAK, Uhlen M, Artursson P. Endogenous gene and protein expression of drug-transporting proteins in cell lines routinely used in drug discovery programs. *Drug Metab Dispos* 2009;**37**:2275−83.